Experiments and geometrical shock dynamics simulations of shock focusing behavior

H. Liu, B. Katko, J. Zanteson, V. Eliasson

Department of Structural Engineering, Jacobs School of Engineering, University of California San Diego, La Jolla, CA 92093, USA

B. Lawlor, C. McGuire, L. Zheng

Department of Mechanical and Aerospace Engineering, Jacobs School of Engineering, University of California San Diego, La Jolla, CA 92093, USA

V. Eliasson: eliasson@ucsd.edu

Abstract Shock wave focusing can lead to extreme thermodynamic conditions at the focal region. However, shock wave focusing is not just a phenomenon that occurs in laboratory settings, but also in nature, and this topic is therefore of interest to different disciplines ranging from astronomy to biomedical devices. In this study, experiments of shock wave focusing are combined with numerical simulations to better understand the interaction between multiple curved shock fronts. In particular, this study concerns shock waves with a decay of flow properties behind the shock front and their interaction during a shock (blast) wave focusing scenario. The experiments are performed using a novel exploding wire setup that can be tailored to produce either cylindrical shocks (in two dimensions) or spherical shocks (in three dimensions). The numerical simulations are performed using geometrical shock dynamics. Results show that the experimental setup can successfully be used to study shock interaction between multiple shocks coalescing into each other. The numerical results show that the undertaken approach using geometrical shock dynamics can closely replicate results obtained solving the full Euler equations of gas dynamics.

1 Introduction

Experiments featuring shock wave focusing provides a controlled environment in which one can study effects of high temperatures, high pressures, high densities, or the interaction of shock waves. Oftentimes, the experimental equipment needed to do so is not prohibitively expensive so these setups are highly suitable for research laboratories in academia or at national laboratories. Typically, horizontal shock tubes are used, and oftentimes these setups feature a constant cross section area such that the conditions behind the shock front remain constant for an extended period of time. However, if the cross section are is increased, or if the shock wave exits the shock tube and is allowed to expand radially, the conditions behind the shock front will decay in an exponential manner. This is also the case for explosives, intentional or unintentional, that expand into the surrounding media.

When a shock interact with another shock, two scenarios can happen: (1) the shocks meet and a regular reflection takes place, meaning a two-shock system is developed containing the incident shock(s) and the reflected shock(s); and (2) the shocks meet and an irregular reflection takes place in which a three-shock system is developed. At this time, there is the incident shock, the reflected shock and a Mach stem. The transition criteria from regular to irregular shock wave reflection depends on the shock medium, the shock Mach numbers, and the geometry of the shock waves. Transition criteria for two-dimensional shock waves with constant properties behind the shock front have been developed, and an excellent summary is provided in [1] with newer updates in [2].

The first experiments on shock wave focusing were performed by Perry and Kantrowitz [3]. Their experiments were executed in a horizontal shock tube setup featuring a teardrop insert at the end of the shock tube. As the shock wave propagated down the shock tube, it split up into a toroidal shape when encountering the tear-drop insert and then had no where else to go but to focus onto itself. Optical observations were made, and light was seen as the shock wave reached the focal region. Since then, many researchers have studied shock wave focusing, e.g. [4, 5]. An overview of the current body of shock wave focusing studies, with introductions to the experimental methods used and the results obtained is presented in [6].

In this study, particular interest was placed upon creating tools that allows for the the investigation of regular to irregular transition regime of two- and three-dimensional shock waves.

2 Experimental setup

The current experiments were performed using a newly designed exploding wire system coupled with an ultra-high-speed camera (Shimadzu HPV-X2) and a z-folded schlieren setup. The exploding wire setup was designed to pass a controlled amount of energy through a very thin metal wire to create shock waves of varying strengths in two or three dimensions. Exploding wire setups are by no means novel in the world of experiments, but have been used since the late 1700s [7] in a number of different studies. Interestingly, these types of setups have also been used in the area of shock dynamic studies. Perhaps most notably are the experiments performed by Ernst Mach on shock reflections in the late 1870s [8] where he was able to deduce the existence of Mach stems based on the pattern left behind by the shock waves on sooted plates.

Here, the work is focused on exploring irregular to regular shock wave reflections for shocks with decaying flow properties behind the shock front. Thus, the experimental setup was designed to be modular so that future research directions can easily be incorporated [9] without needing to redesign the experimental system. The experimental setup consists of four main parts: a charging circuit; a load circuit; a damping circuit; and a triggering mechanism [10]. The setup was built on top of a cart so that it could be wheeled around in the laboratory in a convenient manner. The capacitor bank consists of four capacitors (0.22 µF, General Atomics, Part No. 31160) connected in parallel charged using a DC highvoltage source (50 kV, Glassman High Voltage Inc., Model No. FJ50N2.4). The damping circuit consists of three main parts: the same capacitor bank as in the charging circuit, a switch, and resistors. The resistors (1 k Ω , Pulse Power and Measurement (PPM) Ltd., Series 508AS) are connected in series and facilitate a quick capacitor discharge. The load circuit consists of the capacitor bank, a spark gap switch (10-65 kV, Hofstra Group, Item No. 3114) and exploding wires placed inside a test section. A Rogowski coil (Pearson Electronics) connected to the positive side of the exploding wire is used to trigger the high-speed camera (HPV-X2, 10,000,000 frames per second). The two-dimensional test section setup is shown in Fig. 1(a), and the three-dimensional test section setup is shown in Fig. 1(b). All experimental high-speed photography results were obtained through the utilization of a z-folded schlieren system [11].

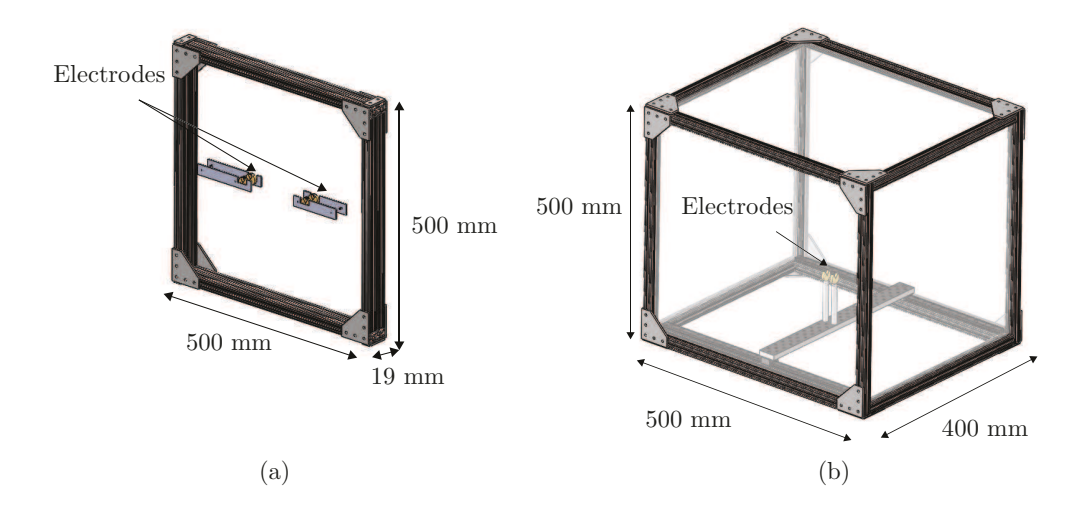


Figure 1: (a) Model of the two-dimensional test section with PMMA windows (inner test section dimension). The inside gap in between the two PMMA windows is 19 mm. Each exploding wire is held in place using two circular brass electrodes with a v-shaped notch. (b) Model of the three-dimensional test section with polycarbonate windows. Each exploding wire is held using two tower structures that are equipped with circular brass electrodes that contain a v-shaped notch at the top of the tower.

3 Experimental results

Figure 2 shows four images from a sequence of an expanding shock wave in the two-dimensional test section. Utilizing the two-dimensional test section and a 0.05-mm diameter nickel chromium wire with a load current of $20~\rm kV$, the resulting images are schlieren photographs taken at a corresponding frame rate of 500,000 frames per second using the Shimadzu high-speed camera.

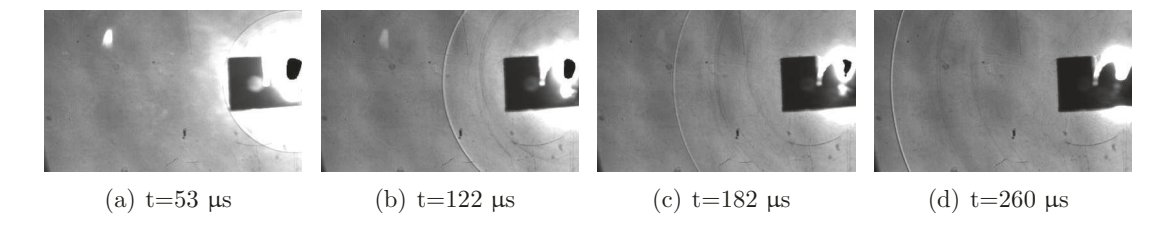


Figure 2: Schlieren photographs taken during an experiment in the two-dimensional test section. The shock wave is propagating from the right to the left. Photographs are taken with the electrical PT-55 trigger using 20 kV. The resolution is 400×250 pixels and the viewing area is approximately 130×80 mm². Time instant zero is when the camera is triggered.

Four photographs from a three-dimensional experiment is shown in Figure 3. Two 0.05-mm-diameter nickel chromium wires were exploded at a capacitor charge voltage of 20 kV. The wires were spaced 76 mm (3 in) from one another and the resulting shock

wave interaction was observed. The schlieren photographs in Figure 3 are taken at a frame rate of 500,000 frames per second. This experiment validates the ability of the experimental setup to visualize the regular (two-shock system) to irregular (three-shock system) interaction of two three-dimensional shock waves.

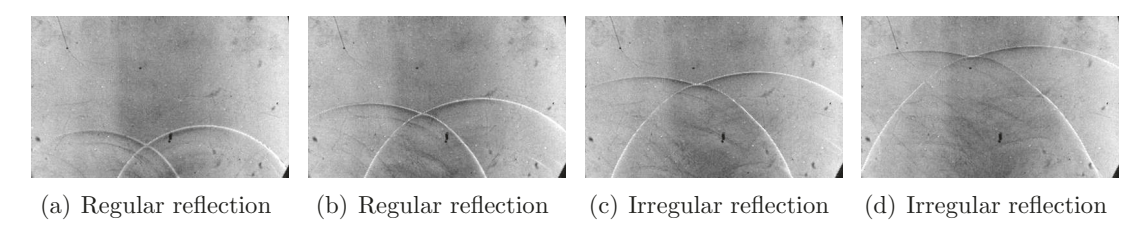


Figure 3: Schlieren photographs taken during an experiment in the three-dimensional test section where two exploding wires are exploded at the same time. The resulting shock waves are propagating from the bottom to the top with the intersection point in the middle of the photograph. The resolution is 400×250 pixels and the viewing area is approximately $130 \times 80 \text{ mm}^2$.

A Matlab script is used to remove optical distortions in the photographs after they have been recorded. Then, the individual shock fronts are tracked and radius versus time information is obtained. From this, velocity fits can be calculated for all experiments. An example of radius versus time plots for four different capacitor voltages (10kV, 13kV, 16kV and 25kV) is shown in Fig. 4. Automation of this process is faster and more accurate than trying to obtain this data by hand.

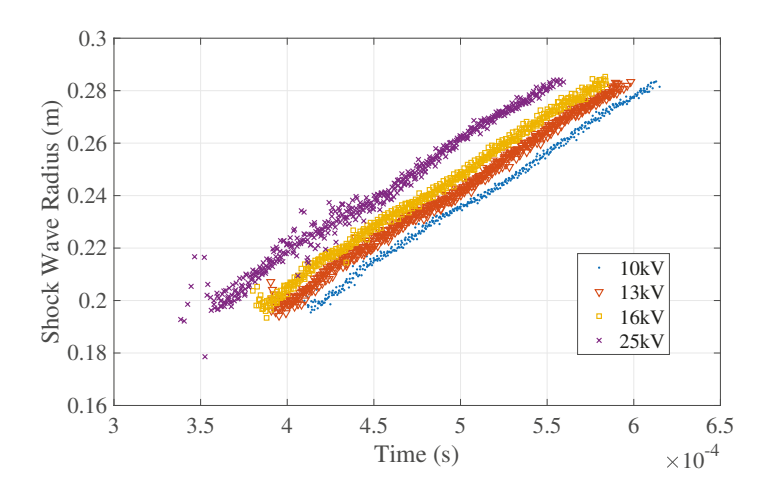


Figure 4: Radius versus time for four different capacitor voltages.

4 Numerical simulations

For this work, the numerical simulations were developed with an end goal of having a fast code to perform optimization simulations with, thus the choice of Geometrical Shock Dynamics (GSD) [12, 13]. Here, we present an investigation into the accuracy of the GSD method used in this work.

Compared to the Euler simulations of gas dynamics, which solve the equations of conservation of mass, momentum and energy, that provide a solution to the entire fluid field, geometrical shock dynamics – as a particle method – only tracks the motion of the shock front. Therefore, the complexity of the problem is lowered and the simulation turnaround time is significantly reduced. However, such advantage comes at the expense of accuracy when blast waves are of interest. A blast wave induces a non-uniform flow state behind the shock front that leads to the invalidation of the underlying assumption of the Area-Mach number relation that the shock motion should be independent of the flow conditions behind the shock front, on which the original GSD theory depends. In fact, a complete form of GSD was derived by J.P. Best [14], shown in Eqs. (1)-(2) next,

$$\frac{d\vec{x}}{dt} = a_0 M \vec{n},\tag{1}$$

and

$$d_{t}M = \frac{-a_{0}M}{d_{M}p + \rho a d_{M}u} \left[\left(\frac{\rho a^{2}u}{a+u} \right) \frac{A'}{A} + \left(\frac{1}{a+u} - \frac{1}{a_{0}M} \right) Q_{1} \right]. \tag{2}$$

Here, the post-shock flow effect term, Q_1 , is incorporated and it models the non-uniformity behind the shock front. The original Area-Mach number relation is just a special case of these equations where this post-shock flow term is simply set to zero. Here, M is the Mach number, A a local area containing the point (x, y), A' = dA/dn is the spatial derivative in the normal direction at that point, a_0 is the speed of sound ahead of the shock front, a is the speed of sound, a is the particle velocity, a is the pressure and a is the density behind the shock front.

There are at least two ways of expressing the post-shock flow effect term in a complete GSD system. One way is to expand the Q_1 -term as an infinite series leading to a new GSD system consisting of infinite coupled ordinary differential equations that can be truncated at any level to achieve a certain order of completeness. If a 1st-order complete system is solved by a 3rd-order accurate TVD Runge-Kutta method, only a negligible improvement over the original GSD can be observed independent of initial blast strength. The other way is to explicitly express Q_1 as a function of $\frac{d\vec{M}}{dt}$, which is nevertheless one of the unknowns pursued in the GSD system. Another method is to input an existing analytical solution to a single blast propagation for $\frac{d\vec{M}}{dt}$. Then, a complete form of Q_1 can be computed and the problem is closed with a system of two coupled ordinary differential equations as in Eqs. (1)-(2).

5 Numerical simulation results

Figure 5 shows a comparison of an M-R plot obtained from an analytical result, the original GSD, and a modified GSD. Here, it is clear that the modified GSD achieved a very good agreement with the analytical solution.

The reason for the success of the modified GSD in simulating the blast propagation was investigated by recording the evolution of Q_1 . It turned out that, as shown in Fig. 6, the modified GSD is able to compute a more accurate Q_1 than the 1st-order complete GSD when compared to the Euler simulation that is used as a reference. A conclusion about the impact of the post-shock flow effect term in GSD can be made: the completeness of Q_1 determines the accuracy of GSD on blast propagation. If Q_1 is not fully expressed, some information about the interaction between the blast front and flow behind it is missing that results in the loss of accuracy; however, once Q_1 can be calculated based on

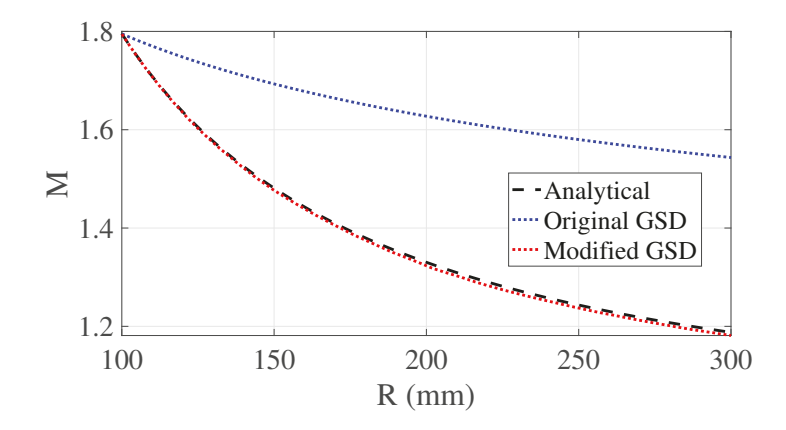


Figure 5: Comparisons of M-R plots of modified GSD, original GSD and the analytical result from [17]

a complete form, the non-uniformity state behind the blast can be correctly accounted for by GSD.

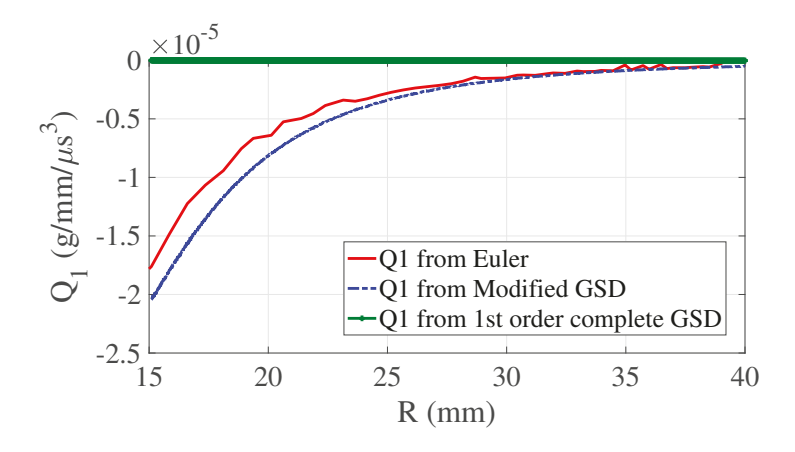


Figure 6: Evolution of the post-shock flow term Q_1 from the modified GSD method.

Several scenarios were then investigated using modified GSD. The simulations were initialized with a successive shock front that represents the combined geometry of multiple blast waves at the transition from regular to irregular reflection. Such transition condition was determined by an analytical model [15] that communicates the sonic criteria [16] to the analytical solution to blast propagation [17] by a straightforward geometry interpretation. The growth and attenuation of Mach stems generated by the interaction of two adjacent blasts were recorded and a good agreement with the Euler simulation was observed.

6 Conclusions

The conclusions can be summarized as follows:

• The novel modular design of the experimental setup and its different test sections successfully allowed for the creation of multiple cylindrical shocks or spherical shocks, which have decaying properties behind the shock front.

- The experimental setup also allows for the study of regular to irregular reflection of cylindrical or spherical shock waves using high-speed photography.
- Geometrical shock dynamics can be used to model an expanding shock wave in two
 dimensions featuring a decay of properties behind the shock front if the post-shock
 term is incorporated into the solver. Here, a two-dimensional code was developed
 in C++, which relies on a third order Runge-Kutta system and mesh regularization
 procedure.
- Different methods to initialize the post-shock flow term were investigated in this work, and results show that this term really matters for the results to be accurate if the flow behind the shock front is not at a constant state for an extended period of time.
- One method to obtain the post-shock term is to use a lookup table in which data obtained either through detailed simulations (e.g. Euler simulations) or experiments for the post-shock flow properties are tabulated to be used at each time step.

Future work include a systematic experimental study to find the point in time and space when regular reflection transitions into irregular reflection for cylindrical and spherical shock waves. Furthermore, the two-dimensional geometric shock dynamics code is being extended to three dimensions.

Acknowledgements

The authors gratefully acknowledge the financial support from the US Air Force Research Laboratory, award number: FA8651-17-1-004, and NSF Fluid Mechanics (CBET), award number: CBET-1803592.

References

- [1] G. Ben-Dor, Shock wave reflection phenomena, Springer, Berlin Heidelberg New York (1991)
- [2] G. Ben-Dor, A state-of-the-knowledge review on pseudo-steady shock-wave reflections and their transition criteria, Shock Waves, 15, 277-294 (2006)
- [3] R.W. Perry, A. Kantrowitz, *The production and stability of converging shock waves*, J.Appl. Phys. **227**, 878–886 (1951)
- [4] K. Takayama, H. Kleine, H. Grönig, An experimental investigation of the stability of converging cylindrical shock waves in air, Exp. Fluids 5, 315–322 (1987)
- [5] M. Watanabe, K. Takayama, Stability of converging cylindrical shock waves, Shock Waves 1, 149–160 (1991)
- [6] N. Apazidis, V. Eliasson, Shock Focusing Phenomena High Energy Density Phenomena and Dynamics of Converging Shocks, Springer Nature, (2018)
- [7] J. McGrath, Exploding wire research 1774-1963, Tech. rep., NRL Memorandum Report 1698, US Naval Research Laboratory (1966)
- [8] J. Blackmore, Ernst Mach; his work, life, and influence, University of California Press, Los Angeles (1972)
- [9] E. Lakhani, Design of exploding wire system, Master's thesis, University of California San Diego (2018)

- [10] W. Mellor, E. Lakhani, J. C. Valenzuela, B. Lawlor, J. Zanteson, V. Eliasson, Design of a multiple exploding wire setup to study shock wave dynamics, in review in Experimental Techniques, (2018)
- [11] C. Wang and V. Eliasson, Shock wave focusing in water inside convergent structures, Int. J. Multiphysics 6, 267–282 (2012)
- [12] G.B. Whitham, Linear and nonlinear waves, Wiley-Interscience (1974)
- [13] W.D. Henshaw, Numerical shock propagation using geometrical shock dynamics, J Fluid Mech 171, 519-545 (1986)
- [14] J.P. Best: A generalisation of the theory of geometrical shock dynamics, Shock Waves 1, 251-273 (1991)
- [15] S. Qiu, Numerical study of focusing effects generated by the coalescence of multiple shock waves, PhD thesis, University of Southern California (2017)
- [16] V. Neumann, Oblique reflection of shocks, Technical Report (1943)
- [17] G.G. Bach and J.H. Lee, An analytical solution for blast waves, AIAA Journal 8, 271-275 (1970)